Available online at www.sciencedirect.com
SCIENCE DIRECT®
Wear 254 (2003) 784–796
WEAR
www.elsevier.com/locate/wear

Friction and wear of low nanometer Si_3N_4 filled epoxy composites

Guang Shi [a], Ming Qiu Zhang [b,*], Min Zhi Rong [a,b], Bernd Wetzel [c], Klaus Friedrich [c]

[a] *Key Laboratory for Polymeric Composite and Functional Materials of Ministry of Education, Zhongshan University, Guangzhou 510275, PR China*
[b] *Materials Science Institute, Zhongshan University, Guangzhou 510275, PR China*
[c] *Institute for Composite Materials (IVW), University of Kaiserslautern, D-67663 Kaiserslautern, Germany*

Received 14 October 2002; received in revised form 6 February 2003; accepted 6 February 2003

Abstract

To prepare epoxy-based composites with low frictional coefficient and high wear resistance, nanometer silicon nitride particles were added. Dry sliding wear tests indicate that the composite materials exhibit significantly improved tribological performance and mechanical properties at rather low filler content (typically less than 1 vol.%). Unlike the severe wear observed in unfilled epoxy dominated by fatigue-delamination mechanism, the wear mode of nano-Si_3N_4 composites is characterized by mild polishing. It is believed that strong interfacial adhesion between Si_3N_4 nanoparticles and the matrix, reduced damping ability and enhanced resistance to thermal distortion of the composites, and tribochemical reactions involving Si_3N_4 nanoparticles account for the reduced frictional coefficient and wear rate of the composites.

Keywords: Nanometer Si_3N_4; Epoxy; Composites; Tribochemical reactions; Interfacial interaction; Damping

1. Introduction

Recent investigations on inorganic nanoparticles filled polymer composites reveal their significant potential in producing materials with low friction and/or high wear resistance [1–7]. In comparison with the widely used micrometer particles, nanoparticles are believed to have the following advantages [3,4]: (i) the mechanical behavior of the bulk materials can be emulated while the abrasiveness of the hard microparticles decreases remarkably as a result of a reduction in their angularity; (ii) the transferred film can be strengthened because the nanoparticles would have the capability of blending well with wear particles; (iii) the material removal of nanoparticulate composites would be much milder than that of conventional composites because the fillers have the same size as the segments of the surrounding polymer chains.

As a continuation of our researches on the improvement of tribological performance of polymer nanocomposites [4,5,7,8], the present paper discusses friction and wear behavior of low nanometer Si_3N_4 filled epoxy composites. It has been known that bulk Si_3N_4 exhibits excellent friction reducing and wear resisting capability owing to the hydrodynamic lubrication effect obtained by tribochemical wear [9]. When Si_3N_4 pin slides against white iron in distilled water, a tribochemical film is formed on the rubbing surface, which protects both Si_3N_4 and iron and makes the paired surfaces smooth [10]. Besides, Si_3N_4 in the form of nano-sized particulates can also provide both thermoplastic and thermosetting polymers with improved tribological properties [1,11]. Wang et al. observed that polyetheretherketone (PEEK) composites containing 7.5 wt.% nano-Si_3N_4 exhibit the highest wear resistance, which is increased by about 85% in comparison with the case of neat PEEK [1]. Similarly, the sliding wear rate of bismaleimide resin against steel counterface is decreased by 72% when 1.5 wt.% nano-Si_3N_4 are incorporated [11]. Considering that the decrement of wear rate of the polymers as a result of the addition of Si_3N_4 nanoparticles is not remarkable enough, the authors of the current work aim at further bringing the effect of nano-Si_3N_4 particles into play and having a deeper understanding of the mechanisms involved as well.

2. Experimental

The epoxy resin used in this study is a low-viscosity diglycidyl ether of bisphenol A with epoxide equivalence weight in the range of 0.48–0.54 mol per 100 g. The curing agent is 4,4′-diaminodiphenylsulfone (DDS). Both the epoxy

* Corresponding author. Tel.: +86-20-84112283; fax: +86-20-84036576.
E-mail address: ceszmq@zsulink.zsu.edu.cn (M.Q. Zhang).

0043-1648/03/$ – see front matter © 2003 Elsevier Science B.V. All rights reserved.
doi:10.1016/S0043-1648(03)00190-X

and curing agent are commercial products of Guangzhou Dongfeng Chemical Co., China, and were used as received without further purification. Nanometer Si_3N_4 particles at a size smaller than 20 nm, produced by Zhoushan Nanomaterials Co., China, were used as the filler. Prior to the composites manufacturing, the nano-Si_3N_4 particles were dried at 120 °C in vacuum for 24 h.

For having an even dispersion of nano-Si_3N_4 in epoxy, both the resin and the fillers with desired proportion were carefully mixed by mechanical stirring and ultrasonication before the curing agent was added at a stoichiometric ratio in respect to the epoxy resin. Then the mixture (consisting of epoxy, the nano-filler and the curing agent) was heated to 130 °C in an oil bath and kept at this temperature for 10 min with stirring to dissolve the curing agent. Finally, the compounds were poured into a polytetrafluoroethylene (PTFE) coated mold, and evacuated for 30 min at 120 °C to remove air bubbles. All the samples were cured following the procedures shown below step by step: 2 h at 100 °C, 2 h at 140 °C, 2 h at 180 °C and 2 h at 200 °C.

Three-point bending tests of the composites specimens were carried out in a Hounsfield universal tester in accordance with GB/T1039-92 standard at a deformation rate of 5 mm/min, while unnotched Charpy impact tests were conducted in a XJJ-5 tester according to GB1843-80(89) standard. Composites' Vickers microhardness was measured by a MARK-3H instrument under a loading of 10 g and holding time of 60 s. Dynamic mechanical analysis (DMA) was made with a TA Instruments (2980 dynamic mechanical analyzer) under frequencies of 1, 3, 10 and 30 Hz from −130 to 250 °C at a heating rate of 5 °C/min. A single cantilever system was used to hold the specimens. Thermomechanical analyses (TMA) of the materials were conducted on the same instrument at a heating rate of 5 °C/min under a constant load.

Unlubricated sliding wear tests were carried out in a pin-on-ring configuration at a constant velocity of 0.4 m/s and pressure of 3 MPa, respectively. The carbon steel ring (0.42–0.45 wt.% C, 0.17–0.37 wt.% Si and 0.5–0.8 wt.% Mn, HRC 50) had a diameter of 40 mm and an initial surface roughness of 0.1 μm. The specimens for wear tests were machined with a geometry of 5 mm × 10 mm × 15 mm, resulting in an apparent contact area of about 5 mm × 10 mm. Prior to wear testing, all the samples were pre-worn to average surface conditions and to reduce the running-in period. The actual steady-state test was conducted for 3 h using the same steel ring as that used for the pre-worn procedure. After that, a weight measurement of the specimens was conducted. Thermal decomposition behaviors of the surface layers of epoxy and the composites pins before and after wear tests were studied by a NETZSCH TG209 thermogravimetric analyzer at a heating rate of 10 °C/min in N_2. Morphologies of the worn surfaces were observed by a JSM-6330F scanning electron microscopy (SEM). X-ray photoelectron spectra (XPS) of the composites' surfaces were recorded by means of a Vacuum Generators Escalb MK II X-ray photoelectron spectrometer with a resolution of 0.8 eV at 240 W (Mg Kα 12 kV). In addition, X-ray energy distribution spectra (EDS) of the counterpart steel rings were collected with a LINK-ISIS 300 apparatus at an accelerating voltage of 20 kV.

3. Results and discussion

3.1. Mechanical properties and interfacial interaction

Incorporation of micrometer inorganic particles into polymers often reduces strength properties of the composites except the stiffening effect. When the bonding between the filler particles and the matrix is poor, tensile strength of a composite is usually lowered with filler content following a power law [12,13]. From Figs. 1 and 2, it may be seen

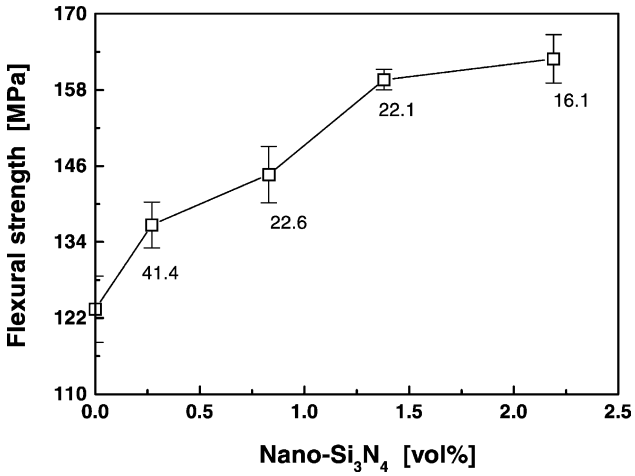

Fig. 1. Flexural strength of nano-Si_3N_4/epoxy composites as a function of filler content. The numerals beside the open square symbols represent the B values calculated according to Eq. (1).

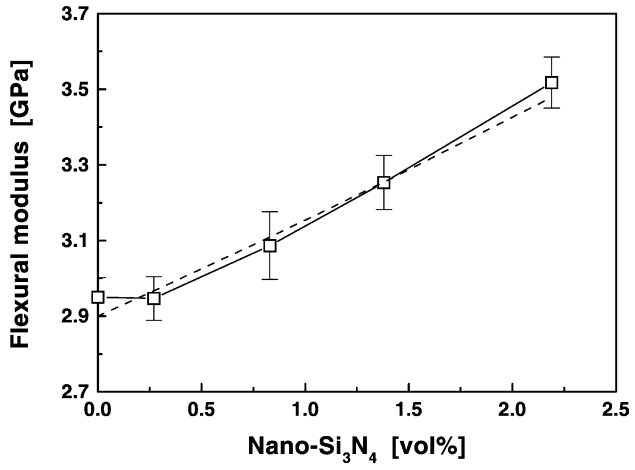

Fig. 2. Flexural modulus of nano-Si_3N_4/epoxy composites as a function of filler content. The dashed line is drawn using Eq. (4) on the assumption that $\Delta R/R = 0.5$.

that the above statements are inapplicable to the current nano-Si_3N_4/epoxy composites. Both flexural strength and modulus increase with a rise in the filler concentration. That means the interfacial adhesion is so strong that the nanoparticles are able to carry the applied load.

Pukánszky considered the case of strong filler/matrix and described the composition dependence of tensile yield stress in heterogeneous polymer systems using a semi-empirical correlation [14]:

$$\sigma_c = \frac{1 - V_f}{1 + 2.5V_f}\sigma_m \exp(BV_f) \quad (1)$$

where σ_c and σ_m denote the yield strengths of the composite and the matrix, respectively; V_f the volume fraction of fillers and B is a parameter related to the interfacial interaction including interlayer thickness and interfacial strength. By using the strength data in Fig. 1 and Eq. (1), a series of B values are obtained and labeled in Fig. 1. In comparison with the work by Walter et al. on Kaolin (0.8 and 1.4 μm) filled high density polyethylene (HDPE) composites, in which the values of B range from 3.8 to 4.35 [15], it is clear that the load bearing areas in the present composites filled with nano-Si_3N_4 are much greater than those in Kaolin/HDPE systems. The nanoparticles have higher reinforcing ability than the micron fillers. On the other hand, the declining trend of the values of B with increasing filler content (Fig. 1) implies that the efficiency of reinforcement of the nanoparticles becomes lower at high filler loading regime, probably due to the worse distribution of the particles in the composites. This is understandable as the more nanoparticles are added into epoxy, the more viscous the mixture and the more difficult the breaking-down of the agglomerated particles.

Kryszewski and Bąk supposed that some volume of the surrounding matrix becomes immobilized as a result of interfacial binding, giving rise to the effective increase in the size of nanoparticles [16]. The effective volume fraction of the partially immobilized material V_e is given by

$$V_e = V_f\left(1 + \frac{\Delta R}{R}\right)^3 \quad (2)$$

where R stands for the radius of nanoparticles and ΔR the increment of the effective particle size. By replacing V_f with V_e in Kerner's equation [17] (Eq. (3)) for a Poisson ratio of 0.5, the elastic modulus of nanocomposites can be described as Eq. (4):

$$E_c = \left[1 + \frac{15V_f(1 - \upsilon_m)}{(1 - V_f)(8 - 10\upsilon_m)}\right]E_m \quad (3)$$

$$E_c = \left[1 + \frac{2.5V_e}{1 - V_e}\right]E_m \quad (4)$$

where E_c is the modulus of the composites, E_m and υ_m the modulus and the Poisson ratio of the matrix, respectively. A comparison between the testing data shown in Fig. 2 and Eq. (4) indicated a good agreement provided $\Delta R/R = 0.5$.

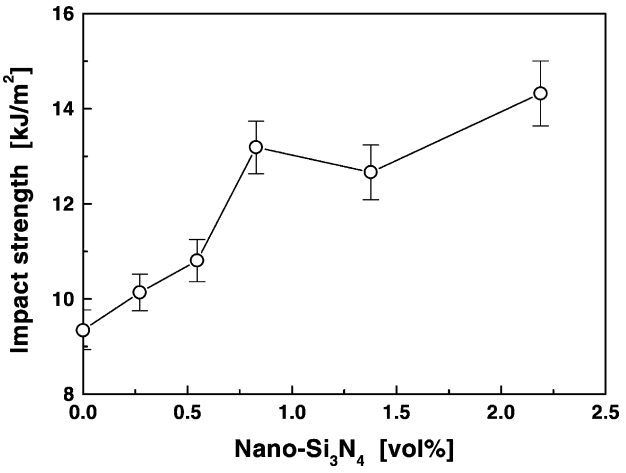

Fig. 3. Unnotched Charpy impact strength of nano-Si_3N_4/epoxy composites as a function of filler content.

It suggests that the effective radius of the immobilized matrix environment surrounding the Si_3N_4 nanoparticles in the current composites is comparable to that of the particles.

In addition to the static mechanical tests, dynamic testing can generate information about the strengthening effect of the fillers from another aspect. As shown by Fig. 3, the impact toughness of the composites increases with nano-Si_3N_4 content. Since unnotched Charpy impact strength reflects the energy consumed before fracture, the results given in Fig. 3 demonstrate that the nanoparticles in the composites are able to induce plastic deformation of the surrounding matrix polymer to a certain extent under the conditions of high strain rate.

Fig. 4 illustrates the mechanical loss spectra of the composites. In contrast to the conventional composites [18], whose damping factor at glass transition, $\tan\delta_{T_g}$, is lower than that of the matrix, the internal friction peak intensity of epoxy shown in Fig. 4 is weaker than the filled versions.

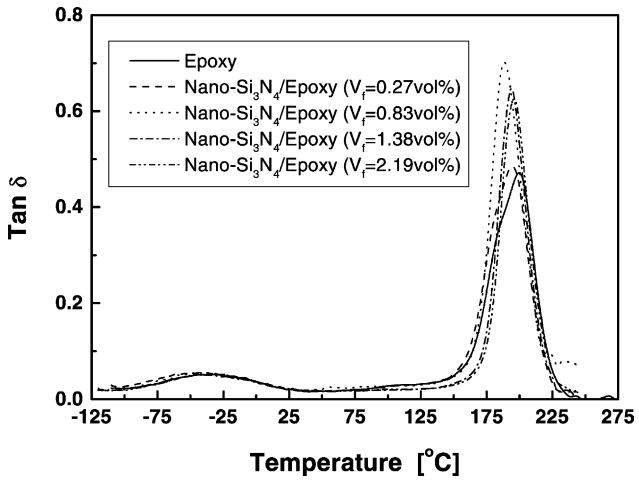

Fig. 4. Temperature dependence of internal friction, $\tan\delta$, of nano-Si_3N_4/epoxy composites measured at 1 Hz.

Table 1
Characterization of β-relaxation of nano-Si_3N_4/epoxy composites

V_f (vol.%)	Peak temperature of β-relaxation (°C)				ΔH_β (kJ/mol)
	30 Hz	10 Hz	3 Hz	1 Hz	
0	−13.8	−22.8	−31.4	−35.9	56.6
0.27	−16.8	−25.2	−33.6	−41.3	75.8
0.83	−19.5	−26.2	−33.2	−41.0	103.6
1.38	−16.4	−22.34	−29.8	−37.6	80.7
2.19	−16.2	−23.8	−30.4	−36.6	78.7

Besides, the glass transition temperature characterized by the α-peak temperature of epoxy is also higher than those of the composites. This phenomenon might result from (i) a weak interfacial interaction in the case of stiff interphase [19] or (ii) a strong interfacial interaction in the case of ductile interphase [20]. Considering that impact tests reveal the ability of the particles to induce plastic deformation, it can be deduced that the latter factor plays the leading role. In fact, this estimation is supported by the calculation of Kubat parameter A [21]:

$$A = \frac{\tan\delta_c}{(1 - V_f)\tan\delta_m} - 1 \quad (5)$$

where $\tan\delta_c$ and $\tan\delta_m$ denote the damping factors of the composites and the matrix, respectively. By using the $\tan\delta_{T_g}$ data of the materials shown in Fig. 4, the values of A for the composites are yielded: 0.04 (V_f = 0.27 vol.%), 0.51 (V_f = 0.83 vol.%), 0.40 (V_f = 1.38 vol.%), and 0.36 (V_f = 2.19 vol.%). As A approaching 0 corresponds to strong interfacial bonding in the composites, it is known that the nanocomposites at the lowest filler fraction (V_f = 0.27 vol.%) has the highest filler/matrix adhesion.

Table 1 further lists the peak temperatures and activation enthalpies of the β-relaxation, ΔH_β, of the composites. The values of the latter parameters were obtained from Arrhenius regression. The β-relaxation has been assigned to motions of the O–CH_2–CHOH–CH_2 hydroxypropylether units and cooperative motions involving hydroxypropylether units and amine crosslinking points that are present in all these systems [22,23]. The greater ΔH_β values of the composites than that of unfilled epoxy induced by the addition of nano-Si_3N_4 means that the particles/matrix interaction is so strong that the motion of alcohol ether in epoxy is greatly obstructed and the crosslinking density is changed to a certain extent as well.

3.2. Friction and wear performance

In general, epoxy is not an ideal material used in sliding wear applications due to its three-dimensional network structure as compared with thermoplastics. As shown in Fig. 5, both frictional coefficient and specific wear rate of unfilled epoxy is quite high. The situation is changed greatly when nano-Si_3N_4 is incorporated. It is seen that there is a significant reduction in the values of μ and $\dot{w}_s$ at filler content as low as 0.27 vol.%. With a rise in the concentration of the nanoparticles, the declining trend becomes gentle and is replaced by a slight increase from 1.38 vol.% on. It means the nanometer Si_3N_4 particles are very effective in improving the tribological performance of epoxy. Although wear data of micrometer Si_3N_4/polymer system are not available in the literature to the authors' knowledge, the result of micrometer SiO_2 particles (18 μm) filled epoxy composites can be cited as Ref. [24]. It is found that the content of micrometer SiO_2 needed to acquire a significant decrease in wear rate of epoxy is as high as 40 wt.%. This is much higher than the amount added into the present systems. In view of applicability, the composites with such a high loading of micrometer particles are far from equaling the nanocomposites characterized by lightweight.

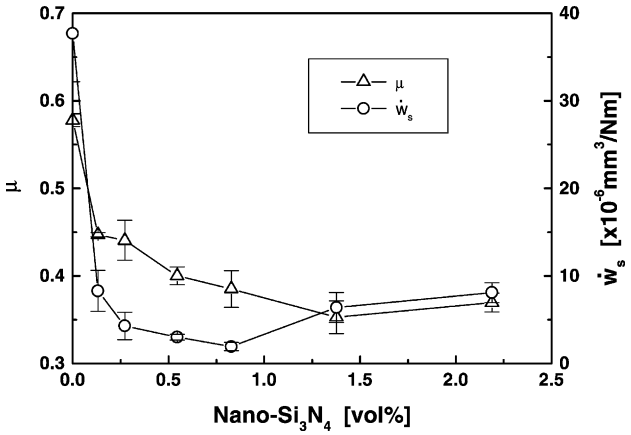

Fig. 5. Frictional coefficient, μ, and specific wear rate, $\dot{w}_s$, of nano-Si_3N_4/epoxy composites as a function of filler content.

Fig. 6 exhibits the SEM micrographs of the worn surfaces of epoxy and the composites. The wear scars on the epoxy pin are characterized by obvious scale-like traces (Fig. 6(a)). A close view (Fig. 6(b)) shows that micrometer size blocks of epoxy resin have left the materials surface. This is indicative for fatigue-delamination generated under repeated loading during sliding. Fatigue wear has been regarded as a main mechanism responsible for the sliding of epoxy against a hard counterpart [25,26]. The model is based on the sub-surface crack nucleation and coalescence due to shear deformation of the softer surface induced by the traction of the harder asperities [27]. For filled composites, the worn surfaces are full of smoothly polished grooves (Fig. 6(c), (e), (g) and (i)). This is particularly evident in the case of V_f = 0.83 vol.% (Fig. 6(e)), which corresponds to the lowest $\dot{w}_s$ as shown in Fig. 5. When the surfaces are observed at high magnification (Fig. 6(d), (f), (h) and (j)), they still look quite smooth besides the thin resin sheets to be removed (Fig. 6(d) and (j)), tiny cracks several nanometers wide and hundreds nanometers long (Fig. 6(f) and (h)), and the exposed nanoparticle agglomerates dozens of nanometer in diameter (Fig. 6(f)). Naturally, the transition from severe wear mode of unfilled epoxy to mild one

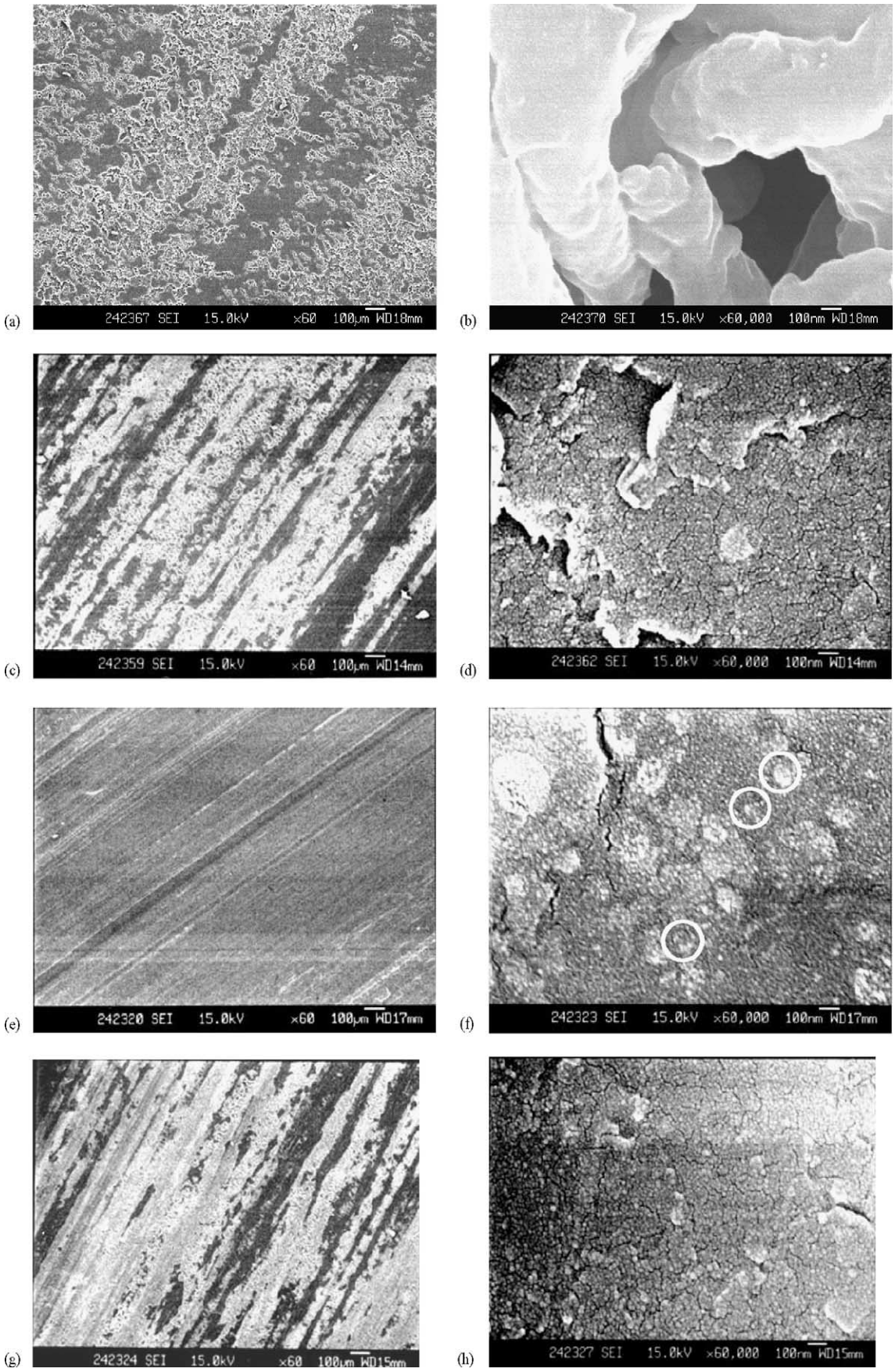

Fig. 6. SEM images of the worn surfaces of (a, b) epoxy, (c, d) nano-Si_3N_4/epoxy composites ($V_f = 0.27$ vol.%), (e, f) nano-Si_3N_4/epoxy composites ($V_f = 0.83$ vol.%), (g, h) nano-Si_3N_4/epoxy composites ($V_f = 1.38$ vol.%), and (i, j) nano-Si_3N_4/epoxy composites ($V_f = 2.19$ vol.%). To ensure equal observation conditions, all the surfaces are examined at two magnifications. The white circles in (f) indicate the agglomerated nanoparticles.

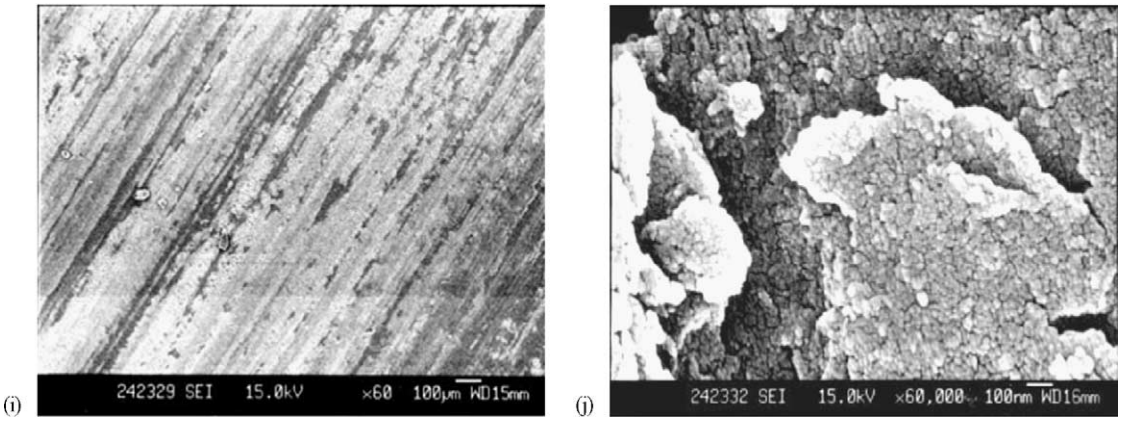

Fig. 6. (*Continued*).

of the composites results from the addition of nano-Si_3N_4 particles.

It has been known from the discussion in last section that the interaction between the nanoparticles and epoxy is quite strong. This should make the detachment of the particles from the matrix rather difficult and thus the amount of material loss is reduced accordingly. However, a careful comparison between Figs. 1–3 and 5 indicates that the filler content dependences of the mechanical properties are not equivalent to those of the tribological performance. Unlike the results in Fig. 5, there is no drastic variation in either strengths (Figs. 1 and 3) or modulus (Fig. 2) with the addition of nano-Si_3N_4. Therefore, other factors in addition to the enhanced nanoparticles/matrix bonding should account for the improved friction and wear properties of the composites.

As surface hardness is generally taken as one of the most important factors that govern the wear resistance of materials, Vickers microhardness, H_v, of the composites is measured (Fig. 7). Evidently, the surface hardness of the composites keeps almost unchanged until the filler content reaches 2.19 vol.%. In fact, the size of the micro-indenter is much larger than that of the nanoparticles. For the composites with lower nanoparticles concentration and better dispersion, the measured H_v values cannot reflect the true hardening effect around the particles but the performance of the matrix resin itself. In the case of higher particulate content (2.19 vol.%, for instance), agglomeration of the particles is rather severe, resulting in higher microhardness with considerable testing error, which also characterizes the uneven distribution of the nanoparticles [4] as confirmed by the decreased reinforcing efficiency at the same filler loading (Fig. 1).

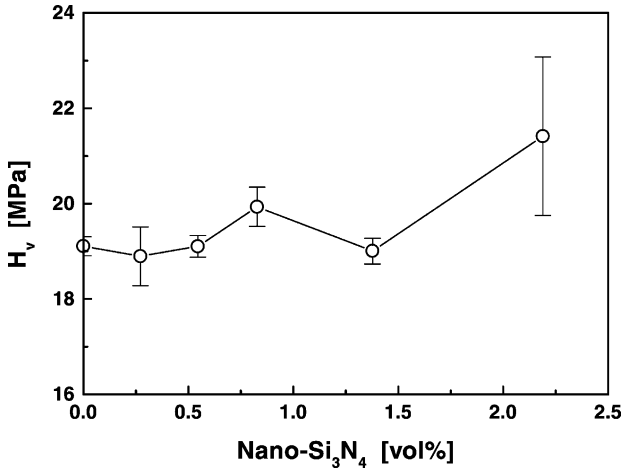

Fig. 7. Vickers microhardness, H_v, of nano-Si_3N_4/epoxy composites as a function of filler content.

Since the measured microhardness is not qualified for analyzing the causes for the reduction of frictional coefficient and wear rate of the composites, the dynamic mechanical responses of the materials (Fig. 4) are studied in correlation with the frictional property as follows. This is done also because of the viscoelastic nature of polymer composites that might influence the tribological behavior of the composites through hysteretic motion of the macromolecular chains. Considering that the transient surface temperature at rubbing surface is rather high, frictional coefficient of the composites is plotted as a function of the area under the α-transition peak in tan δ-temperature (Fig. 8). It is obvious that the relationship follows exponential growth, which is analogous to Arrhenius equation implying the frictional process is closely related to thermally activated motion of the molecular segments of epoxy. Since frictional coefficient increases with a rise in damping of the composites, the ability of the materials to transform mechanical energy into heat contributes to the frictional behavior. In other words, the stiffer the composites, the lower the frictional coefficient, so that the stick-and-slip phenomenon can be prevented [28]. Fig. 9 shows the results of thermomechanical analysis (TMA) of the materials. The comparative measurements manifest that the thermally induced deformation of epoxy is decreased after the addition of the nanoparticles, especially when the filler content is high. It means dimensional stability of the composites is

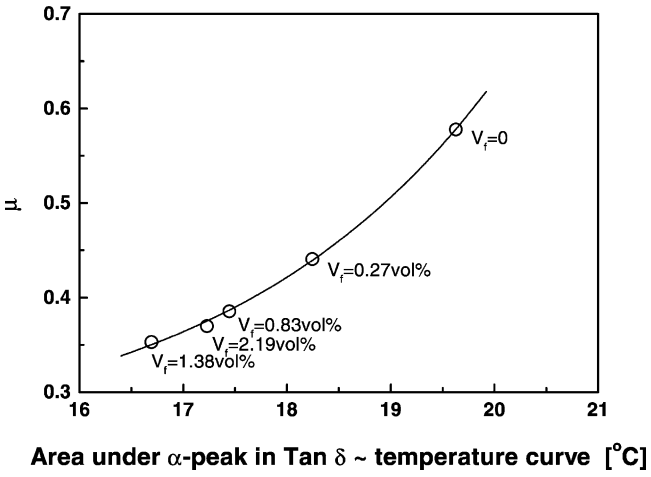

Fig. 8. Frictional coefficient, μ, vs. area under the α-transition peak in tan δ-temperature curve shown in Fig. 4.

superior to that of unfilled epoxy when the specimens are heated up due to the repeated friction, which favors the reduction of frictional coefficient as concluded from Fig. 8.

It is worth noting that when the curve in Fig. 8 is extrapolated to the position at which the α-peak area $= 0$, the corresponding μ does not equal 0. Therefore, mechanical damping is not the only influencing factor. Fig. 10 shows the microhardness values of the surfaces of epoxy and its composites before and after wear testing. Although no obvious variation can be seen in the case of nano-Si_3N_4/epoxy composites, microhardness of the worn surface of epoxy pin decreases significantly, suggesting structural decay of the top resin layer in the scale range of micrometer. On the basis of this finding, thermogravimetric analyses (TGA) of the surface layers of the same samples are carried out to check whether surface chemistry is involved. From Fig. 11 it is seen that both unworn epoxy and nano-Si_3N_4/epoxy composites have similar pyrolytic behavior so that their TGA

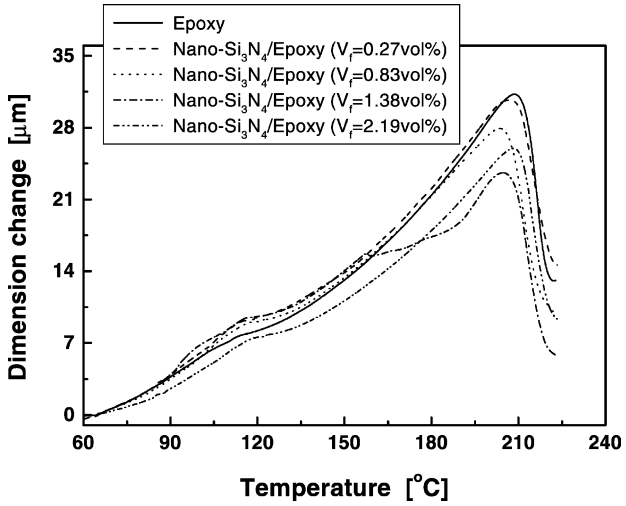

Fig. 9. Thermomechanical curves of epoxy and nano-Si_3N_4/epoxy composites.

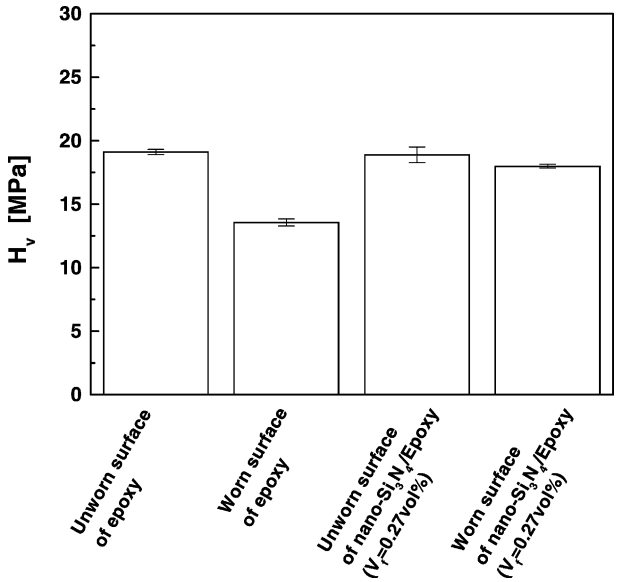

Fig. 10. Vickers microhardness, H_v, of pin surfaces of epoxy and nano-Si_3N_4/epoxy composites before and after the wear tests.

curves almost overlap. When the specimens had undergone sliding wear tests, however, the residual weights of the materials surface layers are much greater than those from the unworn specimens. The disproportional increase in the residual weight strongly suggests transfer from the steel counterpart to the specimen pins besides variation of chemical structures of the components. It is thus necessary to further study the tribochemistry of the worn specimens in the following section.

3.3. Tribochemical analysis

As friction and wear takes place between a pair of counterparts, examination of the surface of the steel ring would be a reasonable starting point. Table 2 records the EDS

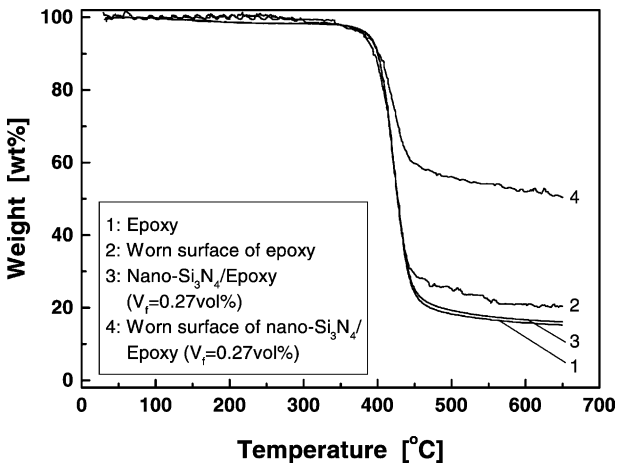

Fig. 11. Thermogravimetric curves of pin surfaces of epoxy and nano-Si_3N_4/epoxy composites before and after the wear tests.

Table 2
EDS analytical results of the surface of the steel counterpart

	Elements and content (%)		
	S	Si	Fe
Steel ring before wear test	0	0.22	98.65
Steel ring rubbed against epoxy pin	0.42	0.21	98.55
Steel ring rubbed against nano-Si_3N_4/epoxy composite pin ($V_f = 0.83\%$)	0.46	1.08	97.82

results of the steel rings before and after rubbing with epoxy and its composites. Having undergone the wear tests, the surface atomic ratios are changed. In the case of epoxy pin, for example, element S appears on the surface of the steel ring. Moreover, the addition of nano-Si_3N_4 into epoxy brings about the rise in the content of Si on the surface of the steel ring. Hence, the above results (Fig. 11, Table 2) evidence the mutual transfer between the specimen pins and the steel rings. To have a clearer image of the tribochemical reaction involved, XPS spectra from the surfaces of epoxy and the nanocomposites should be carefully analyzed.

The low resolution XPS spectra of the pin surfaces of epoxy and nano-Si_3N_4/epoxy composites before and after the wear tests demonstrate that the atomic ratios of C/O have changed (Fig. 12). The increased C/O ratios is indicative of carbonization, as evidenced by the decreased surface microhardness (Fig. 10), manifesting partial chain scission and reorganization of epoxy macromolecules at the surface of the specimen pins during wearing. In consideration of the fact that the frictional surface temperature could be as high as several hundred degrees centigrade in the case of polymer/steel sliding pair [29,30], tribochemically induced structure variation on top layers of the specimens has to take place inevitably [31].

Fig. 13 illustrates the C 1s spectra collected from the unworn and worn surfaces of virgin epoxy and its composites with 0.83 vol.% nano-Si_3N_4. It can be seen that the C 1s peaks from the two worn surfaces (Fig. 13(b) and (d)) are somewhat broadened and shift slightly towards high binding energy regime as compared to those of the unworn surfaces of the materials (Fig. 13(a) and (c)). These phenomena suggest that the carbon atoms become electron-poor. Similar to the C 1s spectra, the O 1s spectra of the samples (Fig. 14) also become broader and shift to high binding energy after sliding wear tests. As a result, it can be estimated that oxidation and carbonization are the main mechanochemical processes that had occurred on the specimen surfaces during wearing driven by the high frictional temperature and contact pressure.

S 2p spectra are given in Fig. 15. The S atom comes from the curing agent in epoxy. Deconvolution of the spectra indicates that a few new peaks appear on the spectra of the worn surfaces, meaning the generation of some S-containing compounds. According to the investigation in Ref. [32], the new compounds are assigned to be FeS, FeS_2 and $FeSO_4$. That is, in the course of sliding wear the S atoms in epoxy

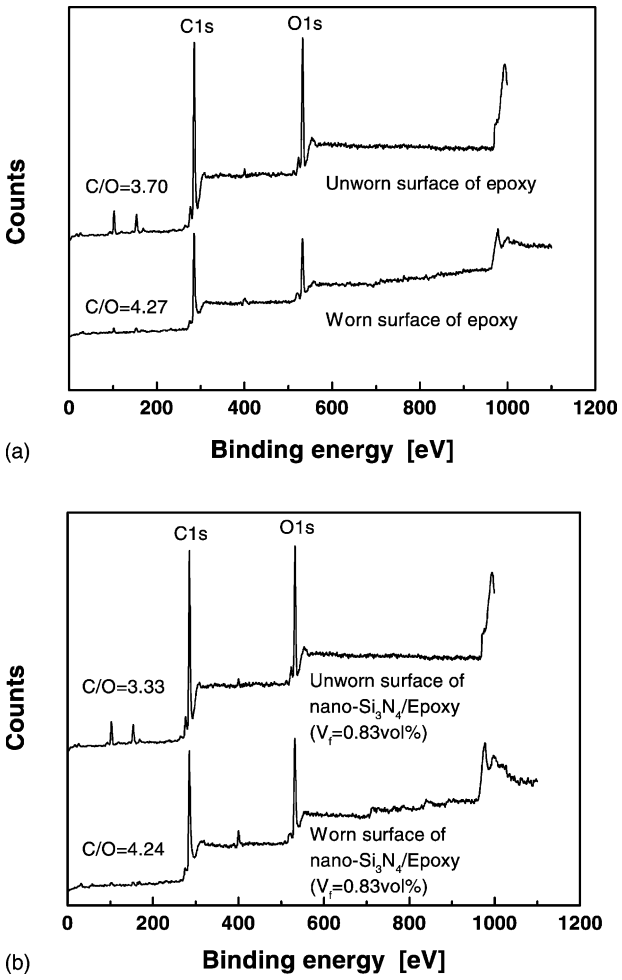

Fig. 12. Low resolution XPS spectra of pin surfaces of (a) epoxy and (b) nano-Si_3N_4/epoxy composites before and after the wear tests.

react with Fe atoms at the metallic counterface and environmental water vapor under high contact temperature and pressure conditions. Then, the new products are attached to both counterfaces, as the trace of S atoms has been found on the steel ring surface (Table 2).

Fig. 16 exhibits the N 1s spectra collected from the sample surfaces. The N atom comes from the curing agent in epoxy and nanometer Si_3N_4 particles in the composites. The spectra collected on the worn surfaces have different profiles from their virgin materials. Besides, the peaks from the worn specimens slightly shift to high binding energy regime, and some new sub-peaks appear. All these imply that the chemical environment of N atoms also becomes more oxidative. The N atoms might react with atmospheric O_2 under sliding wear condition.

Fig. 17 gives the Si 2p spectra of the specimen surfaces. The Si atoms mainly come from the nanometer Si_3N_4 filler in the composites, but those transferring from the polishing paper to the materials' surfaces during samples preparation and from the steel counterpart during wear testing can also contribute to the spectra. The most distinct information

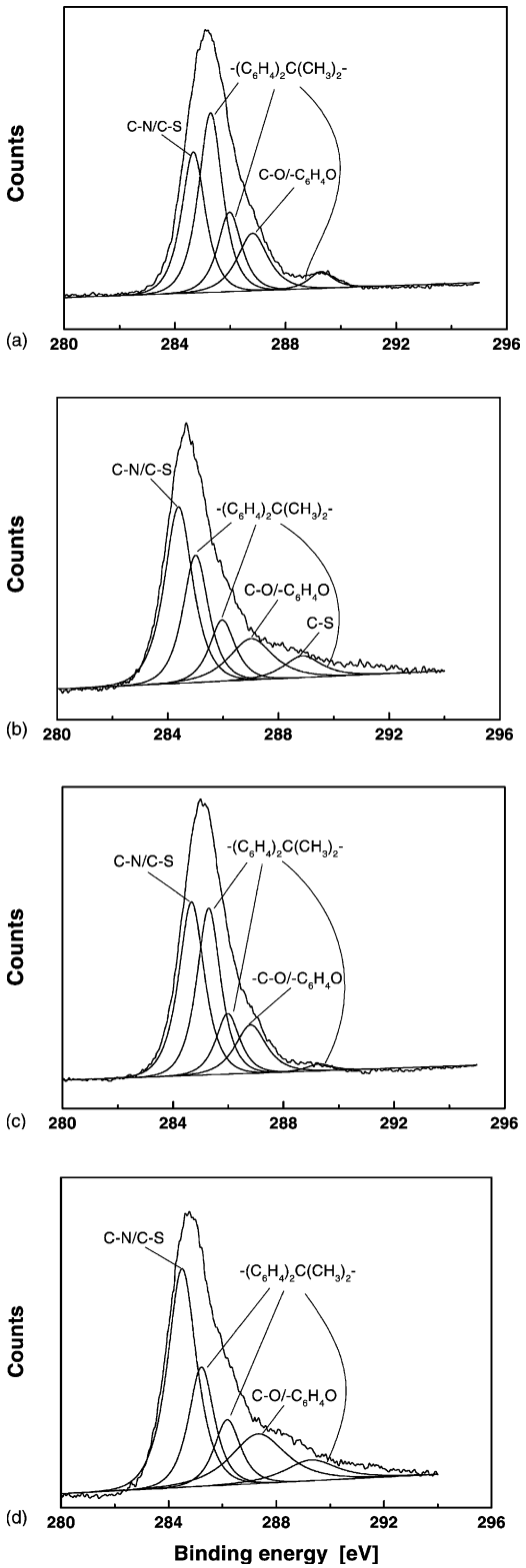

Fig. 13. C 1s spectra of pin surfaces of (a) unworn epoxy, (b) worn epoxy, (c) unworn nano-Si_3N_4/epoxy composites ($V_f = 0.83$ vol.%), and (d) worn nano-Si_3N_4/epoxy composites ($V_f = 0.83$ vol.%).

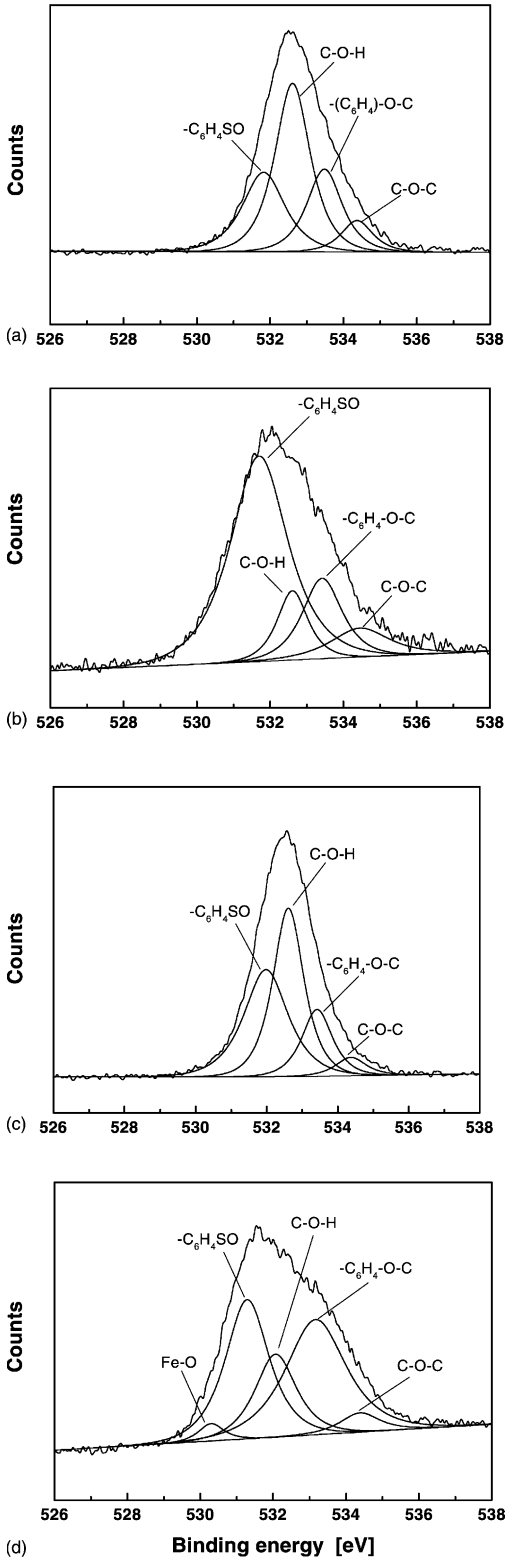

Fig. 14. O 1s spectra of pin surfaces of (a) unworn epoxy, (b) worn epoxy, (c) unworn nano-Si_3N_4/epoxy composites ($V_f = 0.83$ vol.%), and (d) worn nano-Si_3N_4/epoxy composites ($V_f = 0.83$ vol.%).

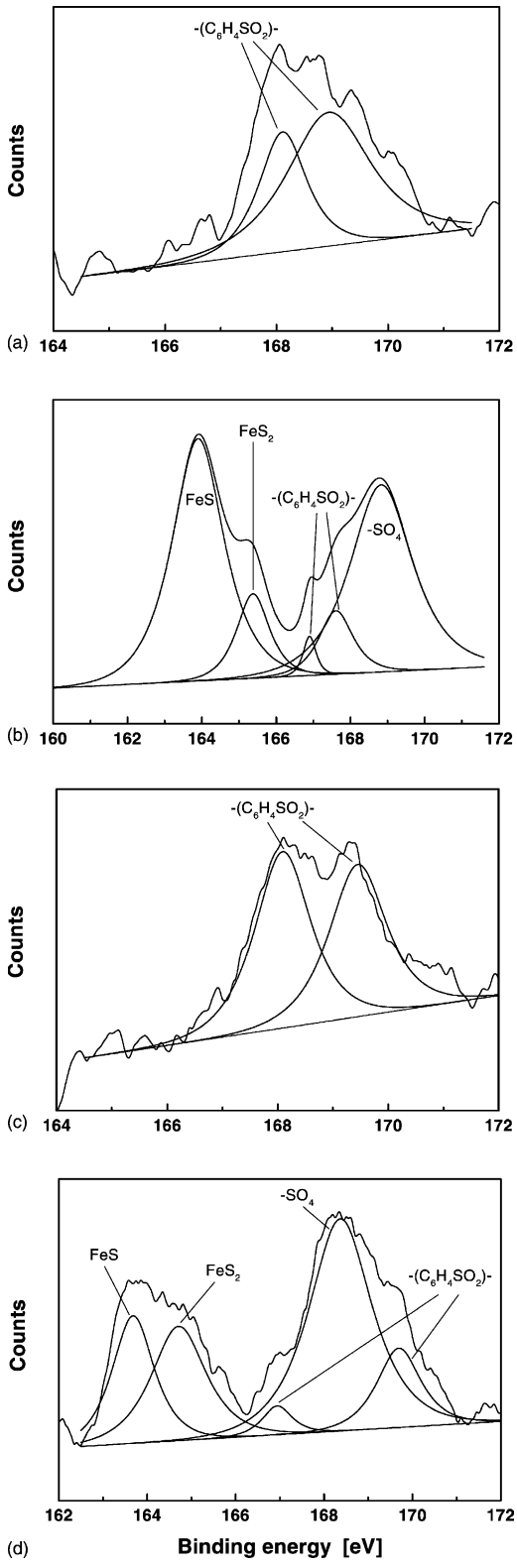

Fig. 15. S 2p spectra of pin surfaces of (a) unworn epoxy, (b) worn epoxy, (c) unworn nano-Si_3N_4/epoxy composites ($V_f = 0.83$ vol.%), and (d) worn nano-Si_3N_4/epoxy composites ($V_f = 0.83$ vol.%).

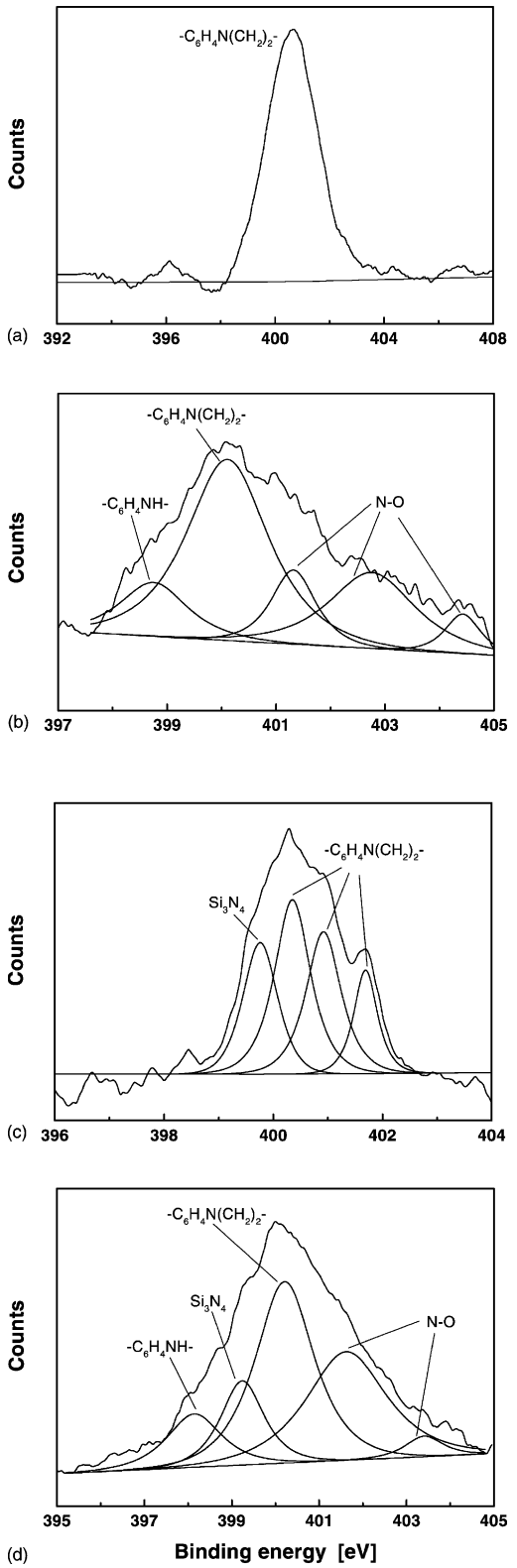

Fig. 16. N 1s spectra of pin surfaces of (a) unworn epoxy, (b) worn epoxy, (c) unworn nano-Si_3N_4/epoxy composites ($V_f = 0.83$ vol.%), and (d) worn nano-Si_3N_4/epoxy composites ($V_f = 0.83$ vol.%).

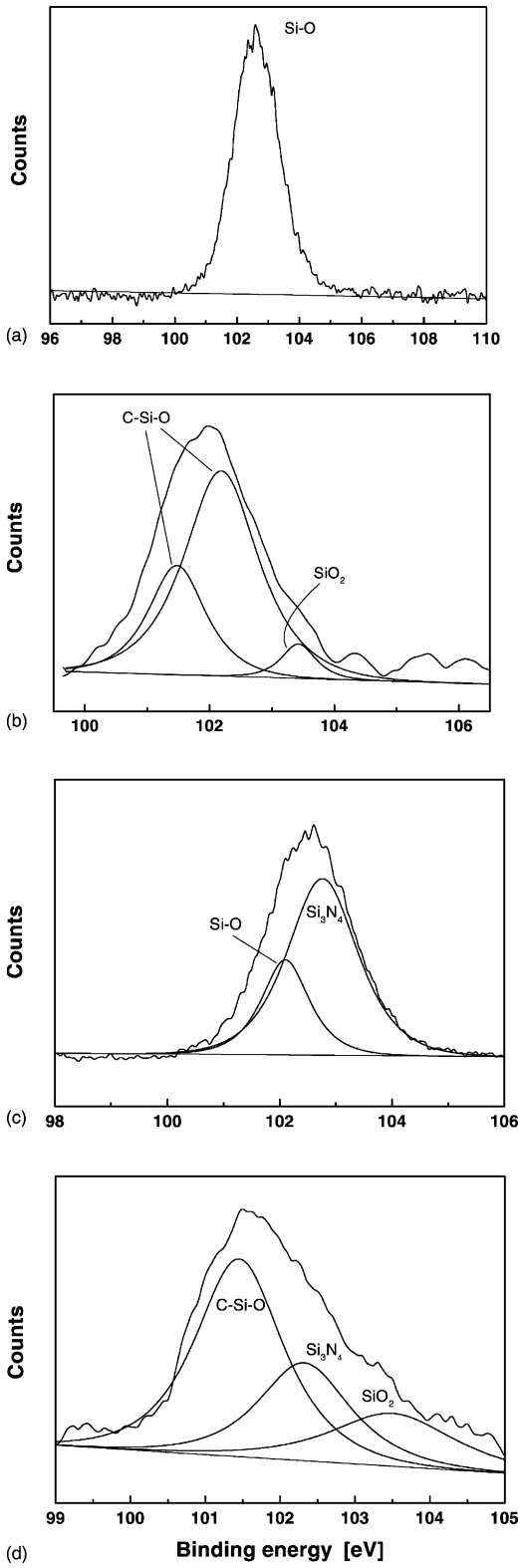

Fig. 17. Si 2p spectra of pin surfaces of (a) unworn epoxy, (b) worn epoxy, (c) unworn nano-Si_3N_4/epoxy composites ($V_f = 0.83$ vol.%), and (d) worn nano-Si_3N_4/epoxy composites ($V_f = 0.83$ vol.%).

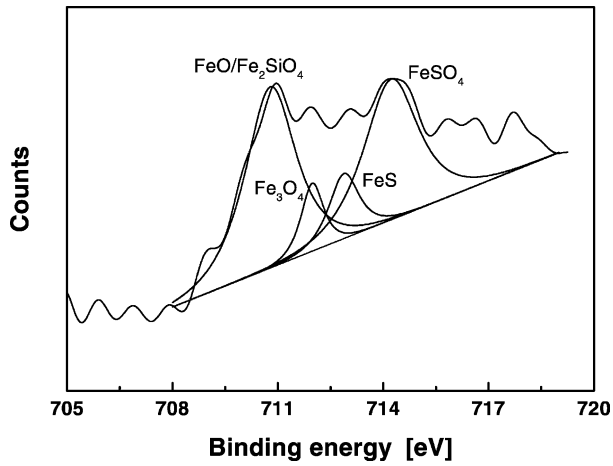

Fig. 18. Fe 2p spectrum of pin surface of worn nano-Si_3N_4/epoxy composites ($V_f = 0.83$ vol.%).

yielded from the spectra before and after wear tests lies in the formation of SiO_2. It represents a tribochemical way of wear in which material is removed molecule to molecule, instead of the classic removal of fragments by fracture [9,33]. In addition, the tribofilm of SiO_2 protects the specimens and the steel counterpart, providing friction reducing ability [10].

Since no Fe peak can be found on the spectra from the pin surfaces of unworn epoxy, worn epoxy and unworn

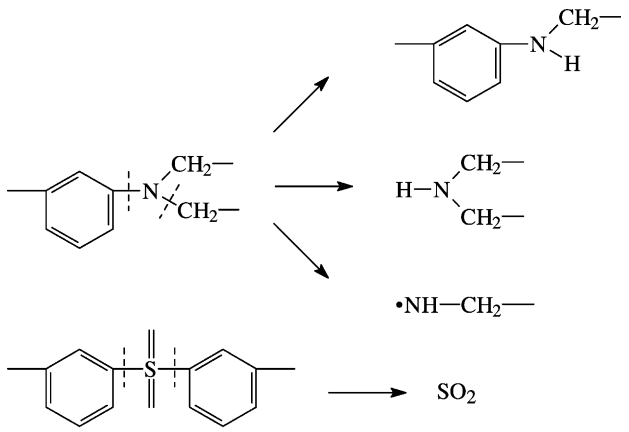

$O_2 + \bullet NH{-}CH_2{-} \rightarrow ON{-}CH_2{-}$

$SO_2 + Fe + O_2 \rightarrow FeSO_4$

$Fe + H_2O + O_2 \rightarrow Fe_3O_4$

$Fe + O_2 + H_2O \rightarrow FeO$

$Fe + S \rightarrow FeS$

$Si_3N_4 + O_2 + H_2O \rightarrow SiO_2$

$Si_3N_4 + Fe + H_2O + O_2 \rightarrow Fe_2SiO_4$

Scheme 1.

Si_3N_4/epoxy composites, Fig. 18 only shows the Fe 2p spectrum collected from the worn surface of the composites. Besides the reactions between the Fe atoms from the metal counterface, the S atoms from epoxy and Si_3N_4, the Fe atoms can also be oxidized, forming FeO and Fe_3O_4. Kong et al. reported on the effect of surface oxide layers on wear behavior [34]. FeO or Fe_3O_4 layers show a significant reduction in friction and wear, while Fe_2O_3 layer promotes the wear. Therefore, the decreasing of μ and $\dot{w}_s$ of epoxy with the addition of Si_3N_4 nanoparticles can be partly attributed to the appearance of FeO and Fe_3O_4 on the counterfaces [35].

To conclude the tribochemical reactions of epoxy and its composites, and those between the materials and the counterface metal Fe, the following scheme is given according to the above discussion, which might help to have an overview of the role of the nanocomposites operating under sliding wear conditions (Scheme 1).

4. Conclusions

1. Incorporation of nano-Si_3N_4 particles into epoxy can significantly reduce frictional coefficient and wear rate of the latter under dry sliding wear conditions. Such an improvement is done at rather low filler content (typically less than 1 vol.%).
2. Strong interfacial adhesion between Si_3N_4 nanoparticles and the matrix, reduced damping ability and enhanced resistance to thermal distortion of the composites, and tribochemical reactions involving Si_3N_4 nanoparticles account for the improved tribological performance of nano-Si_3N_4/epoxy composites.
3. Unlike conventional micrometer particulate composites, flexural strength, flexural modulus and impact strength of nano-Si_3N_4/epoxy composites increase with a rise in filler concentration. This ensures load bearing capability of the composites for practical application in tribological environment, however, there is no straightforward relationship between the mechanical properties and the sliding wear performance of the nanocomposites.
4. As a result of high frictional surface temperature and contact pressure, some chemical reactions that cannot occur under normal circumstances are completed between the sliding counterfaces. The transfer film formed in this way consists of SiO_2 (oxidative products of Si_3N_4), FeO and Fe_3O_4 (oxidative products of Fe), etc., providing self-lubricating effect.

Acknowledgements

The financial support by the Volkswagen-Stiftung, Federal Republic of Germany (Grant no. I/76645), for the cooperation between the German and Chinese institutes on this subject is gratefully acknowledged. Further thanks are due to the National Natural Science Foundation of China (Grant no. 50273047), and the Team Project of the Natural Science Foundation of Guangdong, China (Grant no. 20003038).

References

[1] Q. Wang, J. Xu, W. Shen, W. Liu, An investigation of the friction and wear properties of nanometer Si_3N_4 filled PEEK, Wear 196 (1996) 82–86.
[2] C.B. Ng, L.S. Schadler, R.W. Siegel, Synthesis and mechanical properties of TiO_2-epoxy nanocomposites, Nanostruct. Mater. 12 (1999) 507–510.
[3] C.J. Schwartz, S. Bahadur, Studies on the tribological behavior and transfer film-counterface bond strength for polyphenylene sulfide filled with nanoscale alumina particles, Wear 237 (2000) 261–273.
[4] M.Z. Rong, M.Q. Zhang, H. Liu, H.M. Zeng, B. Wetzel, K. Friedrich, Microstructure and tribological behavior of polymeric nanocomposites, Ind. Lubric. Tribol. 53 (2) (2001) 72–77.
[5] B. Wetzel, F. Haupert, K. Friedrich, M.Q. Zhang, M.Z. Rong, Mechanical and tribological properties of microparticulate and nanoparticulate reinforced polymer composites, in: Y. Zhang (Ed.), Proceedings of the ICCM-13, ID1021, Wan Fang Digital Electronic Publishing, Beijing, 2001.
[6] F. Li, K. Hu, J. Li, B. Zhao, The friction and wear characteristics of nanometer ZnO filled polytetrafluoroethylene, Wear 249 (2002) 877–882.
[7] M.Q. Zhang, M.Z. Rong, S.L. Yu, B. Wetzel, K. Friedrich, Improvement of tribological performance of epoxy by the addition of irradiation grafted nano-inorganic particles, Macromol. Mater. Eng. 287 (2002) 111–115.
[8] M.Q. Zhang, M.Z. Rong, S.L. Yu, B. Wetzel, K. Friedrich, Effect of particle surface treatment on the tribological performance of epoxy based nanocomposites, Wear 253 (2002) 1088–1095.
[9] H. Tomizawa, T.E. Fischer, Friction and wear of silicon nitride and silicon carbide in water: hydrodynamic lubrication at low sliding speed obtained by tribochemical wear, ASLE Trans. 30 (1) (1987) 41–46.
[10] Y.-M. Gao, L. Fang, J.-Y. Su, X.-W. Xu, An investigation on component and formation of tribochemical film in Si_3N_4-white iron sliding pair lubricated with distilled water, Tribol. Int. 30 (1997) 693–700.
[11] H.-X. Yan, R.-C. Ning, X.-Y. Ma, Q.-Y. Zhang, Friction and wear behavior of nanometer Si_3N_4-filled bismaleimide composites, Tribology 21 (6) (2001) 452–455 (in Chinese).
[12] L. Nicolais, M. Narkis, Stress–strain behavior of styrene–acrylonitrile/glass bead composites in the glassy region, Polym. Eng. Sci. 11 (1971) 194–199.
[13] A. Ahmed, F.R. Jones, A review of particulate reinforcement theories for polymer composites, J. Mater. Sci. 25 (1990) 4933–4942.
[14] B. Pukánszky, Particulate filled polypropylene: structure and properties, in: J. Karger-Kocsis (Ed.), Polypropylene: Structure, Blends and Composites, Chapman & Hall, New York, 1995, pp. 1–71.
[15] R. Walter, K. Friedrich, V. Privalko, A. Savador, On modulus and fracture toughness of rigid particulate filled high density polyethylene, J. Adhesion 64 (1997) 87–109.
[16] M. Kryszewski, G.W. Bąk, Reinforcement of elastic polymer matrix filled with ultrafine particles, Acta Phys. Pol. A 92 (1997) 1163–1167.
[17] E.H. Kerner, Electrical conductivity of composites media, Proc. Phys. Soc. B 69 (1956) 802–807.
[18] P.S. Chua, Dynamic mechanical analysis studies of the interphase, Polym. Compos. 8 (1987) 308–313.
[19] H.F. Wu, W. Gu, G.-Q. Lu, S.L. Kampe, Non-destructive characterization of fibre-matrix adhesion in composites by vibration damping, J. Mater. Sci. Lett. 32 (1997) 1797–1798.

[20] M.Z. Rong, M.Q. Zhang, Y. Liu, H.M. Yan, G.C. Yang, H.M. Zeng, Interfacial interaction in sisal/epoxy composites and its influence on impact performance, Polym. Compos. 23 (2002) 182–192.
[21] J. Kubat, M. Rigdahl, M. Welander, Characterization of interfacial interactions in high density polyethylene filled with glass spheres using dynamic-mechanical analysis, J. Appl. Polym. Sci. 39 (1990) 1527–1539.
[22] L. Heux, J.L. Halary, F. Lauprêtre, L. Monnerie, Dynamic mechanical and 13C n.m.r. investigations of molecular motions involved in the β relaxation of epoxy networks based on DGEBA and aliphatic amines, Polymer 38 (1997) 1767–1778.
[23] G.A. Pogany, Gamma relaxation in epoxy resins and related polymers, Polymer 11 (1970) 66–78.
[24] Y. Yamaguchi, Improvement of lubricity, in: Y. Yamaguchi (Ed.), Tribology of Plastic Materials, Elsevier, Amsterdam, 1990, Chapter 3, pp. 143–202.
[25] R. Bassani, G. Levita, M. Meozzi, G. Palla, Friction and wear of epoxy resin on inox steel: remarks on the influence of velocity, load and induced thermal state, Wear 247 (2001) 125–132.
[26] W. Bonfield, B.C. Edwards, A.J. Markham, J.R. White, Wear transfer films formed by carbon fibre reinforced epoxy resin sliding on stainless steel, Wear 37 (1976) 113–121.
[27] N.P. Suh, The delamination theory of wear, Wear 25 (1973) 111–124.
[28] M. Shimbo, M. Ochi, N. Ohoyama, Frictional behavior of cured epoxide resins, Wear 91 (1983) 89–101.
[29] M.Q. Zhang, L. Song, H.M. Zeng, K. Friedrich, J. Karger-Kocsis, Frictional surface temperature determination of high temperature resistant semicrystalline polymers by using their double melting features, J. Appl. Polym. Sci. 63 (1997) 589–593.
[30] M.Q. Zhang, Z.P. Lu, K. Friedrich, Thermal analysis of the wear debris of polyetheretherketone, Tribol. Int. 30 (1997) 103–111.
[31] T.Q. Li, M.Q. Zhang, L. Song, H.M. Zeng, Friction induced mechanochemical and mechanophysical changes in high performance semicrystalline polymer, Polymer 40 (1999) 4451–4458.
[32] L. Yu, S. Bahadur, Q. Xue, An investigation of the friction and wear behaviors of ceramic particle filled polyphenylene sulfide composites, Wear 214 (1998) 54–63.
[33] T.E. Fischer, H. Tomizawa, Interaction of tribochemistry and microfracture in the friction and wear of silicon nitride, Wear 105 (1985) 29–45.
[34] H. Kong, E.-S. Yoon, O.K. Kwon, Self-formation of protective oxide films at dry sliding mild steel surfaces under a medium vacuum, Wear 181–183 (1995) 325–333.
[35] M. Nakamura, K. Hirao, Y. Yamauchi, S. Kanzaki, Tribological behaviour of unidirectionally aligned silicon nitride against steel, Wear 252 (2002) 484–490.